Theoretical Study of the Validity of the Born-Oppenheimer Approximation in the Cl + H_2 → HCl + H Reaction

Millard H. Alexander,[1]* Gabriella Capecchi,[2] Hans-Joachim Werner[2]*

Reactivity of the excited spin-orbit state of Cl with H^2 to yield ground-state HCl products is forbidden by the Born-Oppenheimer (BO) approximation. We used new ab initio potential energy surfaces and exact quantum scattering calculations to explore the extent of electronic nonadiabaticity in this reaction. In direct contrast to recent experiments, we predict that the BO-allowed reaction of the ground spin-orbit state will be much more efficient than the BO-forbidden reaction of the excited spin-orbit state. Also, Coriolis coupling opens up an electronically nonadiabatic inelastic channel, which competes substantially with reaction.

The kinetics of the Cl + H_2 reaction has been the object of study for more than a century (*1*, *2*). The reaction has played an important role in the development of transition state theory, has provided verification of the kinetic isotope effect, and is the paradigm for the reaction of Cl with hydrocarbons, which is of importance in many atmospheric environments. Recently, molecular beam techniques have been used to yield information on this reaction at well-defined collision energies (*2*–*6*). Quasi-classical trajectory and precise quantum scattering investigations have been reported (*7*–*16*) on several potential energy surfaces (PESs) (*17*, *18*). All previous theoretical work has been based on the approximation that only a single PES governs the reaction and that the open-shell character of the Cl atom plays no role in the dynamics.

The approach of molecular hydrogen to an atom in a ^2P electronic state splits the degeneracy of this state, giving rise to three PESs (*18*–*21*). Of these only the lowest, which corresponds to the lower state of A' symmetry in C_s geometry (Σ symmetry in colinear geometry), correlates with the electronic ground state of the products [H + HCl($X^1\Sigma^+$)]. The PESs of the two other states (the higher state of A' symmetry and the unique state of A'' symmetry) correlate with HCl products in the $a^3\Pi$ electronic state, which is considerably higher in energy (*22*) (Fig. 1).

The excited spin-orbit (SO) state of the Cl atom ($^2P_{1/2}$), which lies 880 cm^{-1} (2.52 kcal/mol) above the ground SO state (*23*), does not correlate adiabatically with the electronic ground state of the reaction products. Thus, if the reaction were to proceed adiabatically on a single PES, as would be predicted by the Born-Oppenheimer (BO) approximation, then the excited SO state would not react (*24*, *25*). For the chemically similar F + H_2 reaction, both theory (*21*) and experiment (*26*, *27*) agree that the reactivity of the excited SO state is, at most, 10% of that of the ground state. The Cl + H_2 reaction differs in two respects: (i) the spin-orbit splitting is more than a factor of 2 greater (*23*) and (ii) the barrier height is much higher. The larger SO splitting suggests that the breakdown in the BO approximation would be less important in the Cl + H_2 reaction. However, because the internal SO energy might help to overcome the higher barrier, nonadiabaticity might be more important in Cl + H_2.

In recent molecular beam experiments, Liu and co-workers (*4*–*6*) used two different Cl atom sources to characterize the reactivity of the two SO states of the Cl atom. Except at the lowest collision energies, they conclude that the excited SO state has a substantially larger reactive cross section. This result is surprising, because the body of prior experimental work indicates that BO-allowed (adiabatically allowed) pathways always dominate (*25*, *28*).

This breakdown in the BO approximation inferred by Liu and co-workers (*4*–*6*) demands further theoretical investigation. Two questions must be answered: (i) How large is the reactivity of the adiabatically forbidden channel [Cl($^2P_{1/2}$) + H_2], and (ii) how well can the reactivity of the adiabatically allowed channel [Cl($^2P_{3/2}$) + H_2] be predicted by standard scattering calculations (*7*–*16*), based on a single PES in which nonadiabatic effects are of necessity neglected. We used exact quantum scattering calculations to answer these questions.

We first need accurate PESs for the three electronic states mentioned above. For the subsequent scattering calculations, it is necessary to transform the two states of A' symmetry into an electronically diabatic basis, in which the orientation of the missing 3*p* electron on the Cl atom remains unchanged in the body frame (*21*). Capecchi and Werner (*29*) have carried out internally contracted, multireference, configuration-interaction calculations (*30*, *31*) of these PESs and the SO coupling matrix elements. Transformation into the diabatic basis results in four PESs. Capecchi and Werner subsequently developed multiparameter global fits (*29*) to these

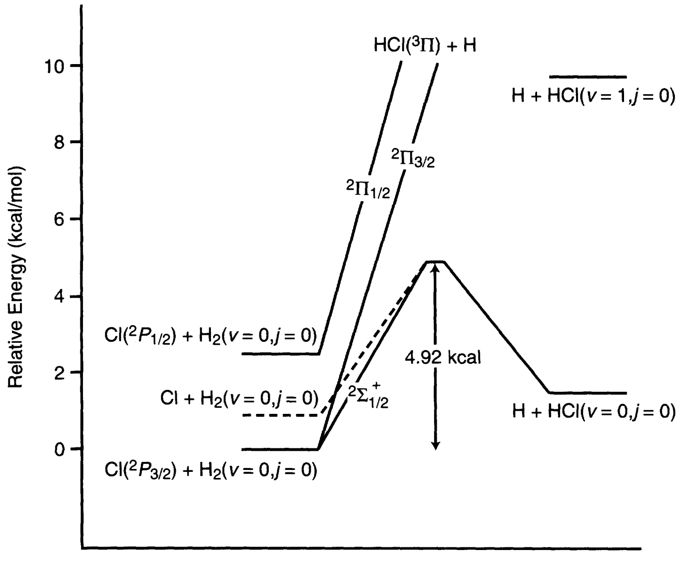

Fig. 1. Schematic plot of the energetics of the Cl + H_2 reaction. The relative reactant energies, the position of the barrier, and the position of the indicated HCl product channels are drawn to scale. All energies include zero-point corrections; those for the barrier were determined from the constants published by Bian and Werner [table II of (*18*)]. Linear-molecule Σ and Π state labels are used, which is appropriate for a colinear transition state. The dashed line indicates the schematic reaction profile for single-surface calculations based on the BW2 PES, in which the SO Hamiltonian is not included.

---

[1] Department of Chemistry and Biochemistry and Institute for Physical Sciences and Technology, University of Maryland, College Park, MD 20742–2021, USA. [2] Institüt für Theoretische Chemie, Universität Stuttgart, D-75069 Stuttgart, Germany.

*To whom correspondence should be addressed. E-mail: mhaaumd.edu (M.H.A.); werneratheochem.uni-stuttgart.de (H.-J.W.)

PESs and to the two SO coupling functions (*21*). Their calculations extend the earlier work of Bian and Werner (*18*), which was limited to the lowest electronically adiabatic ClH_2 PES.

In the Cl + H_2 arrangement, there are six electronic states. These correspond to the three spatial orientations of the 3*p* hole on the Cl atom and the two possible spin-projection quantum numbers. In each H + HCl product arrangement, we neglect the high-lying Π states of HCl (*22*). In general, outside the reactant arrangement, the description of the Cl + H_2 system is unchanged from the original BW2 fit (*18*), which was limited to the lowest electronically adiabatic PES.

If the sum of the electronic interaction Hamiltonian plus the SO coupling in the 6 × 6 electronic basis is diagonalized at each value of the coordinates, the lowest root will define what we will call the fully (electronic + SO) adiabatic Capecchi-Werner (CWad) PES and corresponds to the reactive PES illustrated schematically in Fig. 1. This PES differs from the BW2 PES (*18*), which is obtained by diagonalizing only the electrostatic Hamiltonian, without inclusion of the SO Hamiltonian.

The SO Hamiltonian couples the reactive PES ($^2\Sigma_{1/2}$ in linear geometry) with the two repulsive PESs ($^2\Pi_{3/2}$ and $^2\Pi_{1/2}$ in linear geometry). Because the latter are so much higher in energy at the barrier, inclusion of the SO coupling has a negligible effect at the barrier. However, inclusion of the SO coupling in the asymptotic reactant region lowers the lowest adiabatic PES by ≈1/3 the SO splitting of the Cl atom. Thus, when compared to the BW2 PES, the barrier to reaction on the CWad PES is ≈0.84 kcal/mol higher (*18*, *21*, *32*–*34*).

In addition to the electrostatic and SO Hamiltonians, it is also necessary to determine matrix elements of the orbital angular momentum of the triatomic system $\mathbf{L}^2 = (\mathbf{J} - \mathbf{l} - \mathbf{s} - \mathbf{j})^2$, where *J* is the total angular momentum, *j* is the rotational angular momentum of the diatomic moiety, and *l* and *s* are the electronic orbital and spin angular momenta (*21*).

With the required ClH_2 PESs in the diabatic basis, it is possible to carry out complete quantum scattering calculations. We draw from the formalism presented by Schatz on the Cl + HCl exchange reaction (*32*) and use the algorithms and computer program developed over the past decade by Manolopoulos and co-workers (*35*, *36*), extended, as we have described previously (*21*), to treat abstraction reactions involving an atom in a ^2P electronic state. The choice of integration parameters was identical to those adopted in the single-state studies of the Cl + H_2 reaction (*14*).

We obtain, at each value of the total angular momentum *J*, probabilities for transition from a given initial state to any particular final state of either the reactants (an inelastic collision) or products (a reactive collision). By summing the latter over all accessible product states and averaging over the rotational (2*j* + 1) and electronic ($2j_a + 1$) degeneracy of the initial state (j_a = 3/2 or 1/2), one extracts a total probability for reaction.

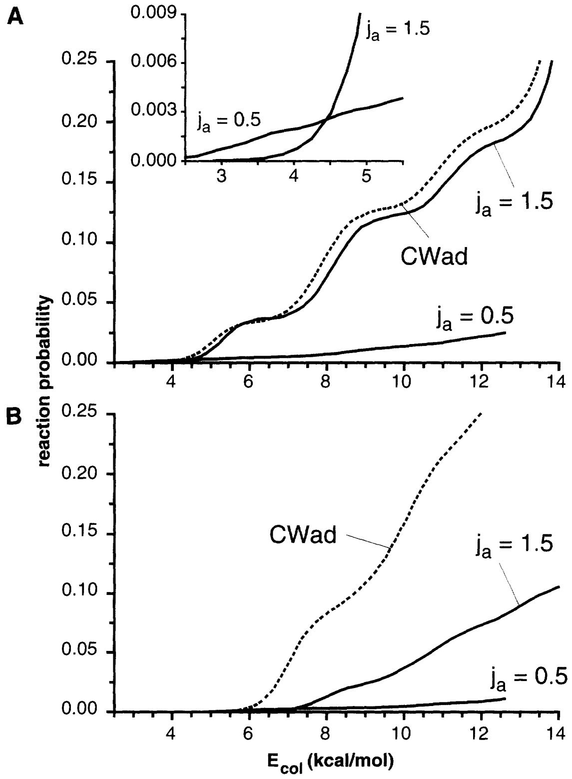

Fig. 2. (**A**) Probabilities for reaction of Cl in the j_a = 3/2 ($^2P_{3/2}$), and j_a = 1/2 ($^2P_{1/2}$) SO states with H_2 (*v* = *j* = 0) for *J* = 0.5. The abscissa is the collision energy. Also shown are reaction probabilities determined from single-state calculations based on the fully adiabatic (CWad) PESs for *J* = 0 but divided by a factor of 2. (Inset) The low-energy behavior of the multistate probabilities. (**B**) Similar reaction probabilities, but for *J* = 17.5.

In Fig. 2 we compare, at the lowest value of the total angular momentum (*J* = 0.5), the calculated total probabilities for reaction of H_2 in *v* = 0, *j* = 0 (the lowest rotational level of *para*-H_2). The multistate results, determined with the full set of diabatic PESs, are compared in Fig. 2 with the *J* = 0 transition probabilities, as predicted by single-state calculations on the CWad PES. In the latter calculation, both the SO and electronic-orbital angular momenta of the Cl atom were neglected, as in any standard single-state treatment of a triatomic reaction (*13*, *14*, *35*, *36*). The reaction probabilities are plotted as a function of collision energy, which is the fundamental dynamical variable in a molecular beam experiment. Thermal rate constants could then be obtained by integration over a Maxwellian distribution of collision velocities, although an equally valid expression involves integration over the total (collision + internal) energy of the "cumulative reaction probability" (*32*).

In the multistate treatment, four states correlate with the ground-state reactants Cl($^2P_{3/2}$) + H_2; namely, as seen in Fig. 1, $\Sigma_{\pm 1/2}$ and $\Pi_{\pm 3/2}$. Of these, the Π states are unreactive, within the BO approximation, so that, to zeroth order, only 50% of the reactants will approach on a PES that leads to reaction. However, in the single-state calculations, one assumes that all (100%) of the reactants will approach on the reactive PES. To take into account this fundamental difference, previous investigators (*21*, *37*) have divided the single-state results by a factor of 2 to compare with the cross sections and probabilities for reaction out of the j_a = 3/2 level of a ^2P atom obtained from multistate calculations.

The probability for (adiabatically forbidden) reaction out of the excited (j_a = 1/2) SO state of Cl is much smaller than the probability for the adiabatically allowed reaction of the ground SO state. Only at collision energies below the zero-point corrected barrier to reaction [E_{col} < 4.93 kcal/mol (Fig. 1)] does the adiabatically forbidden channel start to dominate, because the threshold for reaction of the excited SO state is 2.52 kcal/mol lower.

We also observe that the reaction probabilities predicted by single-state calculations on the fully adiabatic CWad PES agree very well with the multistate probabilities for the adiabatically allowed channel. As discussed above, the single-state probabilities have been divided by 2. Because the excited Π states are very high in energy in the region of the barrier, the topology of the barrier, which controls the flux from reactants to products, is virtually identical in the multistate and single-state calculations.

The pronounced staircase-like structure in the reaction probability out of the lower (adiabatically allowed) SO state corresponds to the successive opening of additional vibrational states at the barrier.

The lower panel of Fig. 2 displays similar reactive transition probabilities, but for $J = 17.5$. Again, the CWad probabilities have been divided by 2. At this higher angular momentum, the centrifugal barrier has increased. Consequently, the threshold for reaction occurs at a higher collision energy. At $J = 17.5$, the multistate reactions are now substantially smaller than those predicted by the single-state CWad calculations, even after division by 2. Similar comparisons at other values of J reveal that as J increases, the multistate reaction probabilities become increasingly smaller than the comparable single-state probabilities. Because the discrepancy grows roughly linearly with J, Coriolis coupling would seem to be responsible.

In the single-state calculations, only three outcomes of a collision are possible: (i) elastic scattering, (ii) inelastic scattering on the reactive PES, or (iii) reactive scattering. In the multistate calculations, additional inelastic channels are present for collisions of Cl in its ground SO state with H_2, namely (Fig. 1) (iv) elastic and inelastic scattering on the repulsive ($^2\Pi_{3/2}$) PES; (v) inelastic scattering from the ($^2\Sigma_{1/2}$) PES to the ($^2\Pi_{1/2}$) PES, which will be accompanied by SO excitation of the Cl atom without reaction; and (vi) inelastic scattering from the reactive ($^2\Sigma_{1/2}$) PES back to the $^2\Pi_{3/2}$ PES. The last process will yield Cl in its ground SO state, accompanied by rotational and/or vibrational excitation of the H_2. At low J, these additional inelastic channels do not seem to deplete the reactive scattering, because the single- and multistate reaction probabilities shown in Fig. 2A are virtually identical. However, a difference between the single-state and multistate probabilities for reaction of Cl($^2P_{3/2}$) does emerge as J increases (Fig. 2B). It is the inelastic channels that are responsible for this difference.

We find that the sum of the reactive and inelastic transition probabilities as predicted by the multistate calculations at $J = 0.5$ and 17.5 agrees very closely with a similar sum, but divided by a factor of 2, of the inelastic and reactive probabilities predicted by the single-state CWad calculations at $J = 0$ and 17. Because this agreement is obtained by dividing the single-state results by a factor of 2, we conclude that incoming flux on the repulsive $^2\Pi_{3/2}$ PES (Fig. 1) has an insignificant probability of either reaction (as discussed above) or inelastic scattering.

Because at higher J the summed (inelastic + reactive) probabilities agree whereas the reactive probabilities are significantly lower for the multistate (as compared to the single-state) calculations (Fig. 2), we conclude that, at higher J, the multistate inelastic probabilities must exceed those predicted by the single-state calculations. This is indeed the case, as illustrated in Fig. 3.

At low energy, below the barrier to reaction, the multistate calculations at $J = 17.5$ reveal a pronounced oscillatory structure. This structure is the manifestation of quantum interference between trajectories that undergo an inelastic transition from the less repulsive $^2\Sigma_{1/2}$ PES to the more repulsive $^2\Pi_{3/2}$ PES when the system passes through the zone of strong nonadiabatic coupling as the atoms approach and then again as they recede, having bounced off the barrier to reaction (*38*).

As the collision energy rises above the barrier, the inelastic probabilities predicted by the CWad single-state calculations remain relatively independent of J. However, the multistate inelastic transition probabilities show a pronounced increase. This is a consequence of the presence of an additional electronic channel(s), not present in the single-state calculations.

In a linear molecule, the non-BO coupling between $^2\Sigma_{1/2}$ and $^2\Pi_{3/2}$ states is due to "*l*-uncoupling" (*39*), which arises from the $\mathbf{J}\cdot\mathbf{l}$ term in expansion of the $\mathbf{L}^2$ operator. Further investigation shows that the J-dependent enhancement of the inelastic probabilities in the multistate calculations can be attributed predominately to rovibrational excitation of the H_2 molecule without excitation of the Cl atom and hence corresponds (Fig. 1) to transitions from the $^2\Sigma_{1/2}$ to the $^2\Pi_{3/2}$ PESs.

Integral cross sections are proportional to the sum over J of the transition probabilities weighted by $(2J + 1)$ (*21*). In general, as the collision energy increases, successively greater values of J contribute. Because the multistate reaction probabilities are increasingly depressed at higher J (compared to the single-state probabilities), we expect that the increase of the multistate reactive cross sections with increasing collision energy will be smaller than the prediction from single-state calculations on the CWad PES. This is indeed the case, as shown in Fig. 4.

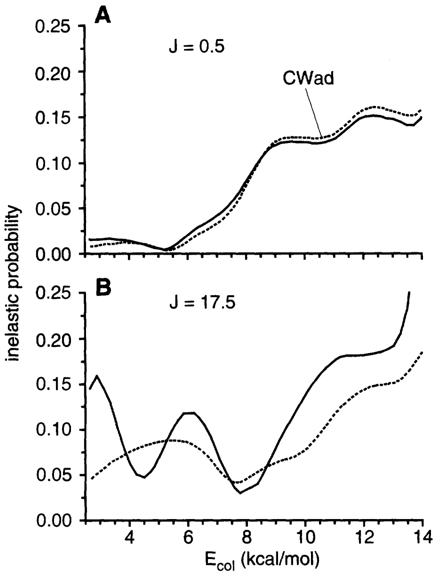

Fig. 3. (**A**) Solid curve indicates the inelastic transition probabilities for Cl($j_a = 3/2$) + H_2($v = j = 0$) for $J = 0.5$, summed over all energetically accessible final states. The abscissa is the collision energy. Dashed curve indicates a similar sum, but divided by 2, of inelastic transition probabilities from single-state calculations on the CWad PES for $J = 0$. The abscissa is the collision energy. (**B**) Similar plot of the inelastic transition probabilities but for $J = 17.5$ ($J = 17$ for the CWad calculations).

In the experiments of Liu and co-workers (*4–6*), only the lowest three ($j = 0$, 1, and 2) rotational levels of H_2 are present in the beam. By weighting the cross sections out of each j level by the experimental populations of these levels, we can obtain reactive cross sections appropriate to the experiments with p-H_2 or n-H_2 (Fig. 5).

We observe, similarly to the transition probabilities, that the cross section for the adiabatically forbidden reaction of Cl in its excited SO state is small in comparison with that for reaction of the ground SO state, which is adiabatically allowed. Only at very low collision energy, where the adiabatically allowed reaction is throttled off by the large barrier, does the adiabatically forbidden reaction begin to dominate. This is a consequence of the greater internal energy of the excited SO state, which does, albeit inefficiently, allow the barrier to be surmounted. Figure 5 is qualitatively similar to our earlier predictions of the relative reactivity of the two SO states of the F atom (*21*).

Because the statistical degeneracy of the ground SO state of Cl is twice as large as that of the excited state, which is not taken into ac-

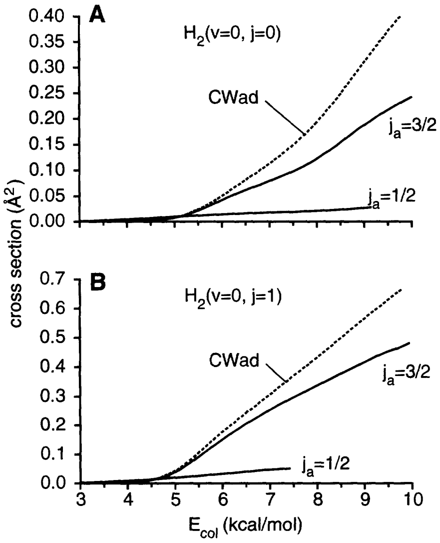

Fig. 4. Integral cross sections for reaction of Cl with H_2($v = 0, j = 0$) (**A**) and with H_2($v = 0, j = 1$) (**B**). Also shown are the predictions of single-state calculations based on the fully adiabatic (CWad) PES, divided by a factor of 2.

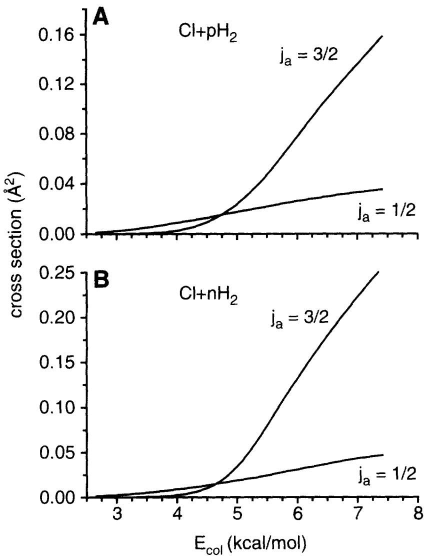

Fig. 5. (**A**) Integral cross sections for reaction of Cl in its ground ($j_a = 3/2$) and excited ($j_a = 1/2$) SO state with p-H_2. (**B**) Similar integral cross sections for reaction with n-H_2. The relative rotational state populations of the $j = 0,1$ and 2 H_2 rotational levels were taken from (*4–6*).

count in Fig. 5, the observed reactivity of the excited SO state will be a factor of 2 less than predicted by Fig. 5.

We predict, fully in agreement with the body of available experimental evidence on other reactions (*25*, *28*), that the adiabatically allowed [Cl($^2P_{3/2}$) + H_2] reaction will dominate the adiabatically forbidden reaction [Cl($^2P_{1/2}$) + H_2], except for collision energies below 5 kcal/mol. This prediction is in direct contrast with the recent work of Liu and coworkers (*4–6*). This disagreement is one of the major currently unsolved problems in the dynamics of elementary chemical reactions.

Although we predict the reactivity of the adiabatically forbidden channel to be small, we conclude that the breakdown in the BO approximation nevertheless plays an important role in the Cl + H_2 reaction. The coupling between the electronic-orbital angular momentum and the overall orbital motion of the reactants opens up a inelastic channel that competes with reaction. The predicted reactive cross sections are smaller than those calculated from more traditional treatments, in which these nonadiabatic inelastic processes are not taken into account.

We have shown that nonadiabatic processes influence the Cl + H_2 reaction dynamics in subtle and as yet not fully understood ways. In the ab initio calculations of Capecchi and Werner, the nonreactive Π states were characterized only in the reactant arrangement, where these states lie relatively close in energy to the reactive Σ state. It may be that additional electronic couplings at (or inside) the reaction barrier underlie the discrepancy with Liu's experiments. The need for further studies, both theoretical and experimental, is clear.

References and Notes

1. T. C. Allison *et al.*, in *Gas-Phase Reaction Systems: Experiments and Models 100 Years after Max Bodenstein*, H.-R. V. J. Wolfrum, R. Rannacher, J. Warnatz, Eds. (Springer, Heidelberg, Germany, 1996), pp. 111–124.
2. P. Casavecchia, *Rep. Prog. Phys.* **63**, 355 (2000).
3. M. Alagia *et al.*, *Science* **223**, 1519 (1996).
4. S.-H. Lee, L.-H. Lai, K. Liu, H. Chang, *J. Chem. Phys.* **110**, 8229 (1999).
5. S.-H. Lee, K. Liu, *J. Chem. Phys.* **111**, 6253 (1999).
6. F. Dong, S.-H. Lee, K. Liu, *J. Chem. Phys.* **115**, 1197 (2001).
7. F. J. Aoiz, L. Bañares, *J. Phys. Chem.* **100**, 18108 (1996).
8. S. C. Mielke, T. C. Allison, D. G. Truhlar, D. W. Schwenke, *J. Phys. Chem.* **100**, 13588 (1996).
9. H. Wang, W. H. Thompson, W. H. Miller, *J. Chem. Phys.* **107**, 7194 (1997).
10. D. Skouteris *et al.*, *Science* **286**, 1713 (1999).
11. U. Manthe, W. Bian, H.-J. Werner, *Chem. Phys. Lett.* **313**, 647 (1999).
12. N. Balucani *et al.*, *Chem. Phys. Lett.* **328**, 500 (2000).
13. B.-H. Yang, H.-T. Gao, K.-L. Han, J. Z. H. Zhang, *J. Chem. Phys.* **113**, 1434 (2000).
14. D. Skouteris *et al.*, *J. Chem. Phys.* **114**, 10662 (2001).
15. F. J. Aoiz *et al.*, *J. Chem. Phys.* **115**, 2074 (2001).
16. C. Shen, T. Wu, G. Ju, W. Bian, *Chem. Phys.* **272**, 61 (2001).
17. T. C. Allison, G. C. Lynch, D. G. Truhlar, M. S. Gordon, *J. Phys. Chem.* **100**, 13575 (1996).
18. W. Bian, H.-J. Werner, *J. Chem. Phys.* **112**, 220 (2000).
19. F. Rebentrost, W. A. Lester Jr., *J. Chem. Phys.* **63**, 3737 (1975).
20. V. Aquilanti, S. Cavalli, D. De Fazio, A. Volpi, *J. Chem. Phys.* **109**, 3805 (1998).
21. M. H. Alexander, D. E. Manolopoulos, H. J. Werner, *J. Chem. Phys.* **113**, 11084 (2000).
22. M. H. Alexander, B. Pouilly, T. Duhoo, *J. Chem. Phys.* **99**, 1752 (1993).
23. C. E. Moore, *Atomic Energy Levels*, NSRDS-NBS 35 (U. S. Government Printing Office, Washington, DC, 1971).
24. K. E. Shuler, *J. Chem. Phys.* **21**, 624 (1953).
25. R. J. Donovan, D. Husain, *Chem. Rev.* **70**, 489 (1970).
26. D. M. Neumark, A. M. Wodtke, G. N. Robinson, C. C. Hayden, Y. T. Lee, *J. Chem. Phys.* **82**, 3045 (1985).
27. M. Faubel *et al.*, *J. Chem. Phys.* **101**, 2106 (1994).
28. P. J. Dagdigian, M. L. Campbell, *Chem. Rev.* **87**, 1 (1987).
29. G. Capecchi, H.-J. Werner, in preparation.
30. H.-J. Werner, P. J. Knowles, *J. Chem. Phys.* **89**, 5803 (1988).
31. P. J. Knowles, H.-J. Werner, *Chem. Phys. Lett.* **145**, 514 (1988).
32. G. C. Schatz, *J. Phys. Chem.* **99**, 7522 (1995).
33. K. Stark, H.-J. Werner, *J. Chem. Phys.* **104**, 6515 (1996).
34. B. Hartke, H.-J. Werner, *Chem. Phys. Lett.* **280**, 430 (1997).
35. J. F. Castillo, D. E. Manolopoulos, K. Stark, H.-J. Werner, *J. Chem. Phys.* **104**, 6531 (1996).
36. D. Skouteris, J. F. Castillo, D. E. Manolopoulos, *Comput. Phys. Commun.* **133**, 128 (2000).
37. F. J. Aoiz, L. Bañares, J. F. Castillo, *J. Chem. Phys.* **111**, 4013 (1999).
38. B. Pouilly, T. Orlikowski, M. H. Alexander, *J. Phys. B* **18**, 1953 (1985).
39. H. Lefebvre-Brion, R. W. Field, *Perturbations in the Spectra of Diatomic Molecules* (Academic Press, New York, 1986), pp. 118–131.

40. M.H.A. is grateful to NSF for support under grant CHE-9971810. H.J.W. was supported by the Deutsche Forschungsgemeinschaft and the Fonds der Chemischen Industrie. G.C. was supported by a fellowship as a participant in the European Union–Training and Mobility of Researchers network 'Reaction Dynamics,' contract no. HPRN-CT-1999-00007. Finally, the authors are grateful to K. Liu and D. Manolopoulos for their encouragement and for many productive discussions.

1 February 2002; accepted 19 March 2002

Dynamic Aggregation of Chiral Spinners

Bartosz A. Grzybowski* and George M. Whitesides*

An object spinning at the surface of a liquid creates a chiral vortex. If the spinning object is itself chiral, its shape modifies the characteristics of the vortex; interactions between that vortex and other vortices then depend on the chirality of the objects that produce them. This paper describes the aggregation of millimeter-sized, chiral magnetized plates floating at a liquid-air interface and rotating under the influence of a rotating external magnetic field. This external field confines all the plates at densities that cause the vortices they generate to interact strongly. For one set of plates investigated, plates of one chirality attract one another, and plates of the other chirality repel other plates of both chiralities.

The properties and interactions of chiral molecules are a central concern in chemistry, with applications in chromatographic separations, asymmetric catalysis, and medicinal chemistry (*1*, *2*). Chiral interactions between molecules are conceptually well understood (*3*, *4*). Interactions between chiral objects larger than molecules are, however, less well explored or exploited. Here, we describe a study of the interactions between millimeter-scale vortices generated in a fluid by the rotation of chiral objects floating at the surface of that fluid. This system has the characteristics that it is dynamic (*5–10*)—that is, the interacting objects (the vortices) exist only when there is a flux of energy into the system—and that both the vortices and the objects that generate them are macroscopic. The system consists of magnetically doped

---

Department of Chemistry and Chemical Biology, Harvard University, 12 Oxford Street, Cambridge, MA 02138, USA.

*To whom correspondence should be addressed. E-mail: bgrzybowskigmwgroup.harvard.edu (B.A.G.); gwhitesidesgmwgroup.harvard.edu (G.M.W.)